The oxidation of sulfides by chromium(V)

Carmela R. Jackson Lepage, Lynn Mihichuk, and Donald G. Lee

Abstract: The mechanism for the oxidation of sulfides by [(me$_4$-salen)Cr^V(O)(pyO)]CF$_3$SO$_3$, where me$_4$-salen is 8,8,8′,8′-tetramethylsalen and pyO is pyridine N-oxide, has been investigated. Results from Hammett correlations on the rates of oxidation of substituted thioanisoles, frontier molecular orbital calculations, and product studies are consistent with a mechanism that is initiated by a single electron transfer to give a radical cation intermediate.

Key words: oxidation, chromium(V), sulfides, radical cation, oxygen transfer.

Résumé : On a étudié le mécanisme d'oxydation des sulfures par le [(me$_4$-salen)Cr^V(O)(pyO)]CF$_3$SO$_3$ dans lequel me$_4$-salen correspond à 8,8,8′,8′-tétraméthylsalène et pyO est un N-oxyde de pyridine. Les résultats de corrélations de Hammett avec les vitesses d'oxydation de thioanisoles substitués, de calculs d'orbitales moléculaires frontières et d'études de produits sont en accord avec un mécanisme qui serait initié par un seul transfert d'oxygène conduisant à la formation d'un intermédiaire cation radical.

Mots clés : oxydation, chrome(V), sulfures, cation radical, transfert d'oxygène.

[Traduit par la Rédaction]

Introduction

The reaction between high valent chromium oxo complexes and sulfides is known to result in the formation of sulfoxides (1). However, the mechanism by which an oxygen atom is transferred from chromium to sulfur in these reactions has not been well defined. By comparison with other similar reactions, there appears to be two primary reaction pathways that should be considered. In one mechanism the reaction would be initiated, as depicted in Scheme 1, by an electron transfer from sulfur to the oxidant, followed by oxygen rebound and solvolysis steps. In this process it is apparent that an intermediate radical cation, **1**, is formed by loss of an electron from sulfur in the initial step.

Alternatively, the reaction could proceed by a concerted oxygen transfer mechanism that does not involve the formation of discrete intermediates, as illustrated in Scheme 2. Although nucleophilic attack on an oxygen atom, as proposed in this scheme, may seem improbable, it should be noted that the process results in a concurrent reduction of the chromium and, therefore, could be regarded as a remote nucleophilic attack on the metal. This process does not involve the formation of intermediate sulfur radicals or cations.

The objective of this work has been to distinguish between these two possible mechanisms for the oxidation of sulfides by a well-characterized chromium(V) complex, [(me$_4$-salen)Cr^V(O)(pyO)](CF$_3$SO$_3$), where me$_4$-salen is 8,8,8′,8′-tetramethylsalen and pyO is pyridine N-oxide. The approach that has been taken is to test for the presence of radical cations by a Hammett analysis applied to the rates of oxidation of substituted thioanisoles, by the use of frontier

molecular orbital calculations, and by a study of the products obtained from the oxidation of sulfides, which would produce radical cations that can react to form aldehydes and disulfides in addition to sulfoxides.

Experimental

The preparation and purification of the sulfides and sulfoxides used in this study have been reported previously (2–4).

Preparation of [(me$_4$-salen)Cr^V(O)(pyO)]CF$_3$SO$_3$

Chromium(II) triflate hexahydrate was prepared from the reaction of chromium metal with triflic acid as follows (5): Trifluoromethanesulfonic acid (9.235 g, 61.54 mmol), obtained from Aldrich, was diluted to 10 mL with distilled and degassed water in a Schlenk tube. Electrolytic Cr chips, size ≤6 mm, purity 99.997% (1.692 g, 32.54 mmol), obtained from AESAR, were added to the Schlenk tube. One of the chips was dipped in perchloric acid and rinsed with water before addition to provide a fresh, clean surface on which the reaction could start. The Schlenk tube was evacuated and back-filled with argon. This mixture was heated to 40°C and left to stir for 7 days. The royal blue solution produced was divided into two portions using cannula techniques and placed in argon-filled Schlenk tubes. Some unreacted Cr chips (0.148 g) were recovered. Water and triflic acid were evaporated in vacuo with the aid of a heat gun, leaving a pale blue solid. The yield, calculated from the amount of unrecovered Cr, was 91.2%. A quartz cell with a side arm Schlenk was used to obtain the UV spectrum of this compound in water. A λ_{max}, observed at 714 nm, corresponds
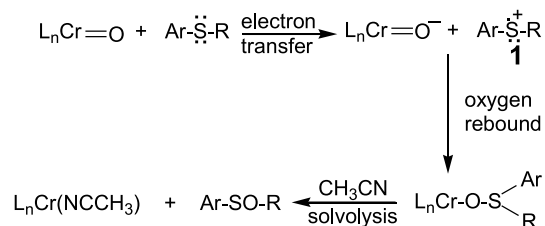
Scheme 1.

Scheme 2.
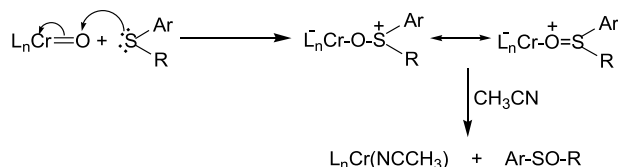
well with that previously reported for chromium(II) compounds (5). There was no maximum at 580 nm corresponding to chromium(III). Since this compound is extremely air-sensitive, it was stored and transferred under argon.

Chromium(II) hexahydrate was ligated with dihydro 8,8,8′,8′-tetramethylsalen (6, 7) and oxidized to the corresponding chromium(III) complex as follows: (me$_4$-salen)H$_2$ (3.570 g, 11.00 mmol) was placed in a 100 mL round-bottom flask fitted with a stopcock. The flask was evacuated and back-filled with argon. Methanol (45 mL), freshly distilled under an argon atmosphere, was added to the flask, and [Cr^{II}(H$_2$O)$_6$](CF$_3$SO$_3$)$_2$ (3.23 g, 7.05 mmol) in an argon-filled Schlenk tube was dissolved in methanol (5 mL) and added dropwise to the round-bottom flask through a cannula. The mixture, initially blue, turned brown. Stirring was continued for 5 h at room temperature. The flask was opened to the atmosphere and heated to reflux for 1 h. The mixture was cooled and the solvent removed on a rotoevaporator. Distilled water (80 mL) was added and the mixture stirred for 2 h. The rusty-orange solid that formed was collected in a Buchner funnel and placed in a 70°C oven to dry overnight. This solid was recrystallized from water giving 2.59 g (4.63 mmol, 65.6%) purified product. The UV and IR spectra compared satisfactorily with literature spectra for [(me$_4$-salen)Cr^{III}(H$_2$O)$_2$]CF$_3$SO$_3$ (6, 8). UV–vis (CH$_3$CN) (nm) (ε (L mol^{-1} cm^{-1})): 418 (3049), 320 (8376), 286 (15 000), 230 (36 000), 202 (25 000). IR (Nujol) (cm^{-1}): 3389–3553 (b), 2954 (s), 2923 (s), 2854 (s), 1618 (s), 1602 (m), 1551 (m), 1465 (s), 1443 (s), 1401 (w), 1379 (m), 1338 (w), 1284 (m), 1238 (s), 1224 (m), 1173 (m), 1146 (m), 1128 (m), 1027 (m), 958 (w), 907 (w), 880 (w), 843 (w), 797 (w), 752 (m), 639 (m).

This chromium(III) complex was oxidized to the corresponding chromium(V) complex by iodosobenzene as follows: [(me$_4$-salen)Cr^{III}(H$_2$O)$_2$]CF$_3$SO$_3$ (1.21 g, 0.37 mmol) was placed in a 100 mL round-bottom flask, and 80 mL of HPLC-grade acetonitrile (CH$_3$CN), obtained from Fisher Scientific, was added along with iodosobenzene (0.60 g, 2.7 mmol), prepared as described in the literature (9). The flask was sealed and the solution stirred. The orange solution that formed initially when the [(me$_4$-

Table 1. Electrospray mass spectral data for [(me$_4$-salen)Cr^V(O)]$^+$.

| Mass | Relative abundance (%) | |
	Theoretical	Experimental
388.11	5.18	5.41
389.11	1.21	2.13
390.10	100.00	100.00
391.11	34.73	35.03
392.11	8.69	9.02

salen)Cr^{III}(H$_2$O)$_2$]CF$_3$SO$_3$ dissolved became greenish-black, indicative of [(me$_4$-salen)Cr^V(O)]$^+$. Prior to rate measurements, any unreacted iodosobenzene was removed by filtration, and pyridine *N*-oxide in acetonitrile was added to produce [(me$_4$-salen)Cr^V(O)(pyO)]$^+$. UV–vis spectroscopic analysis indicated that this was the same complex that had been previously characterized (6).

In addition to UV–vis spectroscopy, the [(me$_4$-salen)Cr^V(O)]$^+$ solution was analyzed using electrospray mass spectrometry (ESI-MS) (10). When the expanded experimental spectrum of the M$^+$ region (*m*/*z* 390) was compared with the theoretical spectrum for C$_{20}$H$_{22}$N$_2$O$_3$Cr$^+$, the isotopic distribution and relative intensities in Table 1 were obtained.

The only mass with a relative abundance that is not within 5% of the predicted value is that of *m*/*z* 389.11. That the resulting abundance, 2.13%, is much greater than the theoretical value of 1.21% is not entirely surprising, since the area of a small peak on the shoulder of a very large peak can be substantially altered by isobaric interferences (11). Overlapping peaks with the same nominal mass can result in a large deviation from the expected value for a small peak. The other isotopic distribution peaks, all within 5% of the expected values, along with a good comparison between the UV–vis spectrum of this complex with that reported for the complex previously characterized (6) provide convincing evidence for its structure.

Kinetic methods

The visible spectrum of a solution of [(me$_4$-salen)Cr^V(O)]CF$_3$SO$_3$ in acetonitrile decreases in intensity uniformly from 350 to 800 nm. However, when pyridine *N*-oxide (pyO) is added to the solution, a broad band centered at 628 nm appears (in accordance with work previously described in the literature (6)). Data summarized in Fig. 1 indicate that the intensity of this band increases as the concentration of pyO is increased. The most reasonable explanation for this observation is reversible ligation with formation of a new complex, [(me$_4$-salen)Cr^V(O)(pyO)]$^+$, when pyridine *N*-oxide is present. Since the absorbance plateaus when the concentration of pyO is 0.1 M or greater, it can be assumed that the equilibrium expressed in eq. [1] lies substantially to the right under such conditions.

[1]   [(me$_4$-salen)Cr^V(O)(CH$_3$CN)]$^+$ + pyO

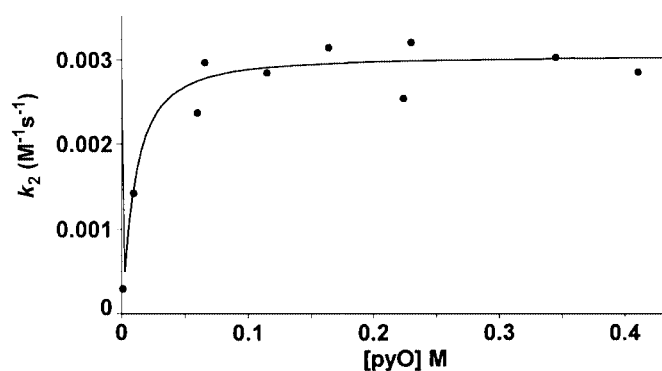$\rightleftharpoons$ [(me$_4$-salen)Cr^V(O)(pyO)]$^+$ + CH$_3$CN
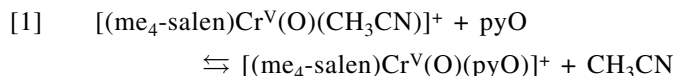
When a reductant is added to these solutions, the band at 628 nm diminishes with time, thus providing a convenient physical change that can be used to monitor reaction rates.

Table 2. Rate constants for the oxidation of methyl *p*-tolyl sulfide.[a]

[Sulfide] (M)	$k_{obs} \times 10^4$ (s^{-1})	$k_b \times 10^5$ (s^{-1})	$k_1 \times 10^4$ (s^{-1})	$k_2 \times 10^3$ (s^{-1} M^{-1})
0.02977	3.009	3.191	2.690	9.04
0.02977	3.080	3.100	2.770	9.30
0.08932	7.877	3.694	7.507	8.40
0.08932	8.146	3.834	7.763	8.69
0.1191	10.76	4.648	10.30	8.65
0.1191	11.54	4.495	11.09	9.31
0.1488	14.22	4.611	13.76	9.25
0.1488	13.68	4.002	13.28	8.92
0.1488	14.00	3.312	13.67	9.19
0.1488	13.60	2.759	13.32	8.95

[a]Temperature = 25°C.

Fig. 1. Dependence of absorbance at 628 nm on pyridine *N*-oxide concentration. $[[(me_4\text{-salen})Cr^V(O)]^+] = 2.58 \times 10^{-4}$ M.
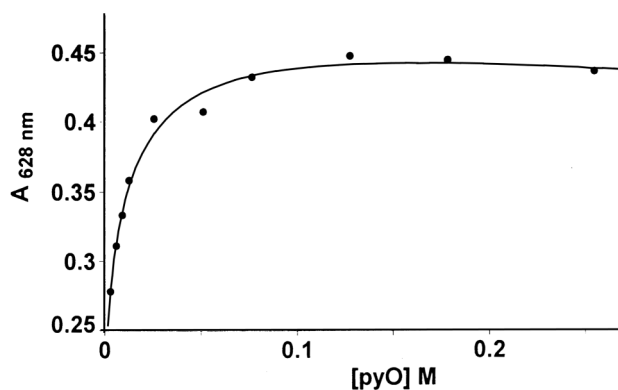
Fig. 2. Pseudo-first-order rate plot for the oxidation of thioanisole. [Thioanisole] = 0.341 M. $[[(me_4\text{-salen})Cr^V(O)(pyO)]^+] = 3.69 \times 10^{-4}$ M. Slope = -1.01×10^{-3} s^{-1}. $r^2 = 0.999$.
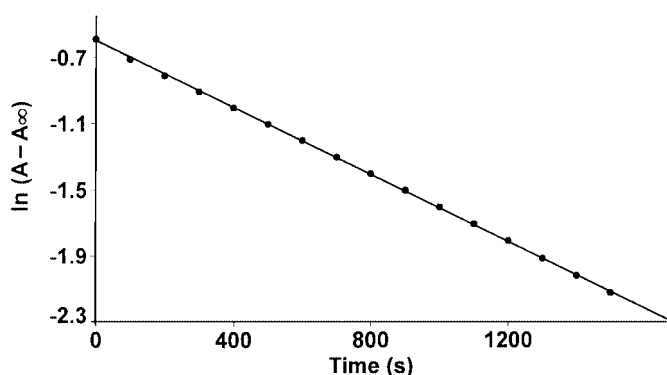
For example, when an excess of thioanisole is added to a solution of $[(me_4\text{-salen})Cr^V(O)(pyO)]^+$, good pseudo-first-order rate plots are obtained (see Fig. 2). The final product exhibits a spectrum identical to that obtained by adding pyridine *N*-oxide to $[(me_4\text{-salen})Cr^{III}(H_2O)_2]^+$. It is necessary to correct the observed pseudo-first-order rate constants, k_{obs}, obtained from the slope of such plots for a slow reduction of the oxidant that occurs in the absence of added reductant. The corrected pseudo-first-order rate constants, k_1, are obtained by subtraction of the rate constant for the corresponding blank reactions, k_b, from the observed rate constant ($k_1 = k_{obs} - k_b$). The observation that the magnitude of k_1 is di-

Fig. 3. Dependence of second-order rate constants on pyridine *N*-oxide concentration. [Thioanisole] = 0.328 M.

Table 3. Effect of added water on rate constants.[a]

[H$_2$O] (M)	$k_2 \times 10^3$ (s^{-1} M^{-1})
0	2.69[b]
0.19	2.64[b]
1.85	2.92[c]

[a][Methyl phenyl sulfide] = 0.341 M; $[[(me_4\text{-salen})Cr^V(O)(pyO)](CF_3SO_3)] = 2.40 \times 10^{-4}$ M.
[b][pyO] = 0.115 M.
[c][pyO] = 1.58 M.

rectly proportional to the concentration of added reductant (Table 2) indicates that the reaction is second order overall — first order in oxidant and first order in reductant.

The effect of pyridine *N*-oxide on the reaction kinetics was determined by measuring the rate constants for solutions containing variable concentrations of pyO. As can be seen from Fig. 3, rates are increased by the addition of pyridine *N*-oxide; however, the effect plateaus at about 0.1 M pyO and above. This result is consistent with the absorbance data in Fig. 1 and the previous suggestion that the equilibrium in eq. [1] must be shifted to the right above 0.1 M pyO. To ensure that the effect of pyridine *N*-oxide would be constant throughout this study, its concentration was maintained above 0.1 M in all experiments, the usual working concentration being about 0.3 M.

In a series of similar experiments it was found that addition of water to the solvent had a negligible effect on the magnitudes of the observed rate constants (see Table 3). It is apparent, therefore, that small amounts of moisture would

Table 4. Rate constants and activation parameters for the oxidation of X-substituted thioanisoles by $[(me_4\text{-salen})Cr^V(O)(pyO)]CF_3SO_3$.

X	$k_2 \times 10^3$ (M^{-1} s^{-1})^a	$\Delta H^{\ddagger}$ (kJ mol^{-1})	$\Delta S^{\ddagger}$ (J mol^{-1} K^{-1})	$\Delta G^{\ddagger}$ (kJ mol^{-1})^a
4-MeO	47.0 ± 1.8	38.0 ± 1.7	–142.9 ± 6.0	80.6 ± 2.5
4-Me	9.88 ± 0.21	49.6 ± 1.0	–117.6 ± 3.2	84.7 ± 1.4
H	3.27 ± 0.31	49.6 ± 1.4	–127.5 ± 4.8	87.6 ± 2.0
4-F	2.23 ± 0.03	51.3 ± 1.5	–123.8 ± 4.8	88.2 ± 2.1
4-Cl	1.49 ± 0.08	64.3 ± 2.7	–83.3 ± 9.3	89.1 ± 3.9
3-Cl	0.607 ± 0.023	53.0 ± 1.7	–128.8 ± 5.7	91.4 ± 2.4

^{a}Temperature = 25.0°C.

Scheme 3.
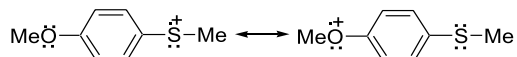
not have an impact on the accuracy of the measured rate constants.

In a typical kinetic experiment, 2.0 mL aliquots of 0.3 M pyO in acetonitrile were added to two 10-mm cuvettes. One cuvette was fitted with a Teflon septa-seal top. Additional solvent (0.1 mL) was added to the other cuvette to compensate for the volume difference that would occur when reductant was added through the septa-seal. An aliquot of freshly prepared oxidant (0.30 mL) was added to each of the cuvettes. They were then flushed with argon for 3 min and sealed. Both cuvettes were placed in the thermostated cell compartment of an HP8452 Diode Array UV–vis spectrophotometer and held at a constant temperature for 29 min. A solution of thermostated and degassed reductant (0.10 mL) was injected through the septa-seal using a microlitre syringe. This cuvette was inverted several times to ensure good mixing and replaced in the thermostated cell compartment. The reaction rates were then monitored at 628 nm. Observed pseudo-first-order rate constants, k_{obs}, were obtained from the data collected from the cuvette containing reductant, and the blank rate constants, k_b, were simultaneously obtained using data collected for the solution in the other cuvette.

Activation parameters

Activation parameters, as defined by application of the Eyring Equation (eq. [2]), were determined by measuring the rate constants at several temperatures and preparing plots of ln k_2/T vs. $1/T$ (12). A typical plot has been reproduced in Fig. 4 and the results are summarized in Table 4. Since both of the proposed mechanisms predict second-order kinetics, the large negative entropies of activation observed are consistent with either Scheme 1 or Scheme 2.

[2] $\ln k_2/T = -\Delta H^{\ddagger}/RT + \Delta S^{\ddagger}/R + \ln k_B/h$

Results and discussion

If a radical cation (see Scheme 1) is formed during the oxidation of substituted thioanisoles, it would be stabilized by substituents that could enter into a direct resonance interaction with it, as depicted in Scheme 3. Since resonance of this type requires interaction of the $3p$ orbitals of sulfur with the carbon $2p$ orbitals of the aromatic ring, it may not make a large contribution to the stability of the radical cation; however, it should be sufficient to cause the rates of oxidation of

Fig. 4. Eyring plot for the oxidation of thioanisole. Slope = -6.04×10^3 K. Intercept = 8.68. $r^2 = 0.996$.
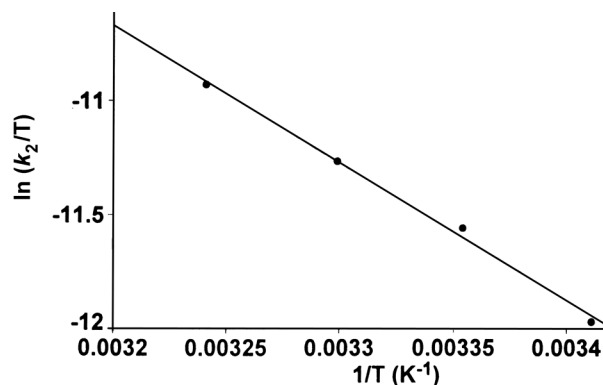
substituted thioanisoles to correlate somewhat better with Hammett σ^+ substituent constants, as compared with the corresponding σ constants. From a comparison of the plots in Figs. 5 and 6, it can be seen that this is, in fact, the case. The correlation is obviously better when σ^+ substituent constants are used.

A similar direct resonance effect for the intermediate proposed in Scheme 2 would require overlap between a sulfur $3d$ orbital and the $2p$ orbitals of the aromatic ring. Therefore, its contribution to the stability of the transition state would be insignificant, and a better correlation would be expected with σ substituent constants, as observed for the oxidation of sulfides by high valent manganese and ruthenium oxides, both of which exhibit better correlations with σ substituent constants (3, 13, 14). This result, therefore, suggests that the oxidation of sulfides by $[(me_4\text{-salen})Cr^V(O)(pyO)]^+$ likely involves the formation of intermediate radical cations as in Scheme 1.
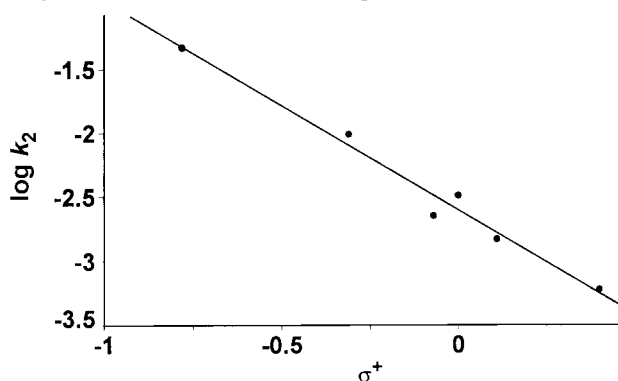
The observation that sulfoxides are not oxidized by $[(me_4\text{-salen})Cr^V(O)(pyO)]^+$ is also consistent with an electron transfer mechanism. Since the electron density at the sulfoxide sulfur would be decreased by polarization of the S=O bond, as in Scheme 4, the activation energy for electron transfer would be greatly increased. Other oxidants such as permanganate and ruthenium tetroxide, which are believed to proceed by a mechanism similar to the one depicted in Scheme 2, oxidize sulfoxides more readily than sulfides (3, 4).

Also consistent with this conclusion is the observation that the rate of oxidation of 4-nitrothioanisole is too slow to measure under these conditions. In this compound the electron density at sulfur is decreased by resonance, as depicted in Scheme 4. Frontier molecular orbital theory predicts that there should be a direct correlation between the energies of

Table 5. Product distributions for the oxidation of substituted benzyl phenyl sulfides by [(me$_4$-salen)Cr^V(O)(pyO)]CF$_3$SO$_3$.
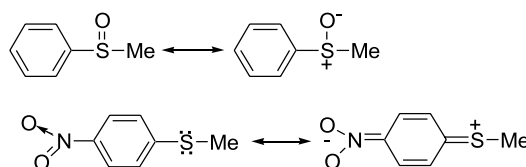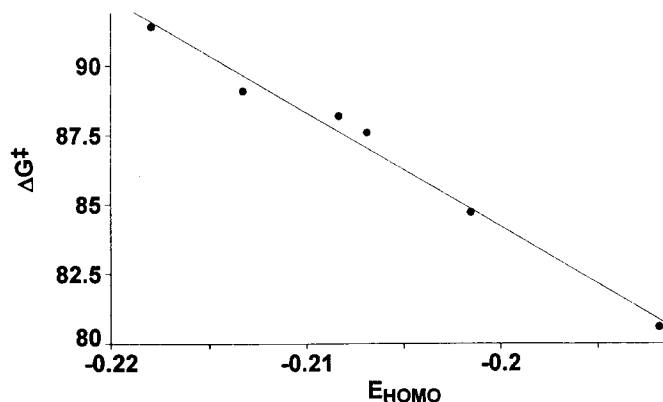
Sulfide	Product Ratios[a]		
	Sulfoxide	Aldehyde	Starting material
Benzyl phenyl sulfide	0.47	—	0.53
4-Methoxybenzyl phenyl sulfide	0.31	0.031	0.66
3,4,5-Trimethoxybenzyl phenyl sulfide	0.16	0.088	0.75

[a]Product ratios were determined, as previously described (2), from the integrals of ^{1}H NMR spectra.

Fig. 5. Hammett correlation with σ-substituent constants. From left to right the substituents are 4-methoxy, 4-methyl, hydrogen, 4-fluoro, 4-chloro, and 3-chloro. Slope = –2.65. r^2 = 0.95.
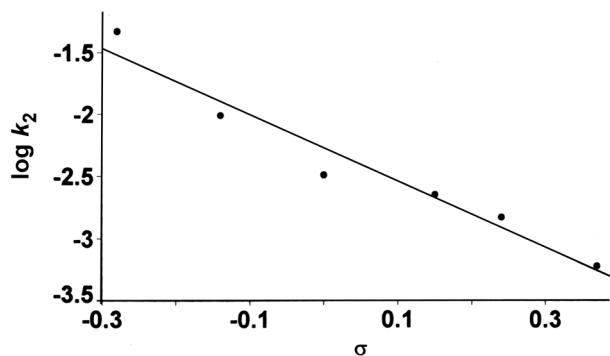
Fig. 6. Hammett correlation with σ$^+$-substituent constants. From left to right the substituents are 4-methoxy, 4-methyl, 4-fluoro, hydrogen, 4-chloro, and 3-chloro. Slope = –1.64. r^2 = 0.98.

Scheme 4.

Fig. 7. Correlation of second-order rate constants with HOMO energies. From left to right the substituents are 3-chloro, 4-chloro, 4-fluoro, hydrogen, 4-methyl, and 4-methoxy. Slope = –410. r^2 = 0.985.

the sulfide HOMOs and the rates of reactions initiated by single electron transfers. Assuming that the LUMO of the oxidant is at a higher energy than the HOMOs of the sulfides, increasing the energy of the HOMO should result in a faster reaction (15). When the energies of the HOMOs of the substituted thioanisoles were calculated at the B3LYP/6-31G* level, a good correlation with activation energies was observed (16) (see Fig. 7). This result is most consistent with the mechanism in Scheme 1 where the reaction is initiated by a single electron transfer.

It is also possible to test for the formation of intermediate radical cations by studying the products formed when methoxy-substituted benzyl phenyl sulfides are oxidized. The radical cations formed from these compounds can react to give aldehydes in competition with the formation of sulfoxides in the oxygen rebound step depicted in Scheme 1 (17–19). For example, reaction of 3,4,5-trimethoxybenzyl phenyl sulfide gives only 3,4,5-trimethoxybenzaldehyde and

diphenyl disulfide when oxidized by cerium(IV) ammonium nitrate, a known one-electron transfer oxidant (2). Previous work has indicated that the formation of aldehydes and disulfides is initiated by loss of a proton from the radical cation to give a free radical, **2**, which is known to be readily oxidized to the corresponding aldehyde, as in Scheme 5. Introduction of the methoxy substituents increases the acidity of the radical cation, promoting proton loss and subsequent aldehyde formation.

When the products obtained from the oxidation of benzyl phenyl sulfide, 4-methoxybenzyl phenyl sulfide, and 3,4,5-trimethoxybenzyl phenyl sulfide were compared, the results summarized in Table 5 were obtained. The product ratios were determined using ^{1}H NMR integrals as previously described (2). These data, which show that the ratio of aldehyde to sulfoxide increases from 0 for unsubstituted benzyl phenyl sulfide to 0.10 and 0.55 for 4-methoxybenzyl phenyl sulfide and 3,4,5-trimethoxybenzyl phenyl sulfide, respectively, are most consistent with the reaction mechanism presented in Scheme 1. Oxidations by high valent manganese and ruthenium oxides, which have been proposed to react by a concerted oxygen transfer, as in Scheme 2, give only sulfoxides and sulfones with these same sulfides (2).

Scheme 5.
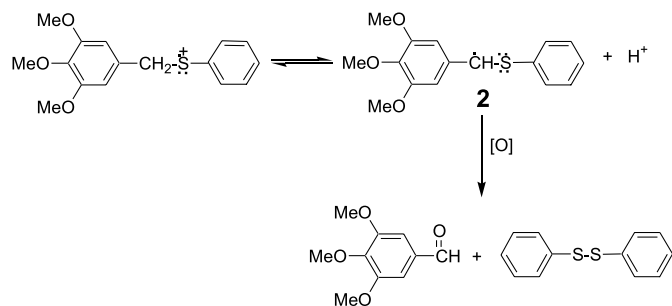
Although any one of these tests individually do not provide compelling evidence for the electron transfer mechanism, the combined impact of the three tests (i.e., the Hammett analysis, the frontier molecular orbital calculations, and the product studies) is convincing, and it appears that the reaction between sulfides and [(me$_4$-salen)Cr^V(O)(pyO)]$^+$ is most likely initiated by a single electron transfer.

It is of interest to note that the oxidation of sulfides by chromium(V) and most other high valent transition metals appears to proceed by different mechanisms. Because the oxidation of proteins and lipids in free radical processes has been associated with the onset of several diseases (20–22), the observed tendency of chromium(V) to react by a one-electron transfer is consistent with the belief that the carcinogenic properties of oxochromium compounds are associated with their tendency to react by free radical oxidation mechanisms. The oxides of manganese, ruthenium, molybdenum, and iron are not carcinogenic, presumably because they react with sulfides by concerted mechanisms that do not involve the formation of intermediate radicals (2, 23).

Acknowledgments

References

1. M. Hudlicky. Oxidation in organic chemistry. ACS monograph 186. American Chemical Society, Washington. 1990. p. 253 and refs. therein.
2. S. Lai, C. Jackson Lepage, and D.G. Lee. Inorg. Chem. **41**, 1954 (2002).
3. N. Xie, R.A. Binstead, E. Block, W.D. Chandler, D.G. Lee, T.J. Meyer, and M. Thiruvazhi. J. Org. Chem. **65**, 1008 (2000).
4. B.L. May, H. Yee, and D.G. Lee. Can. J. Chem. **72**, 2249 (1994).
5. W.H. Tamblyn, E.A. Volger, and J.K. Kochi. J. Org. Chem. **45**, 3912 (1980).
6. K. Srinivasan and J.K. Kochi. Inorg. Chem. **24**, 4671 (1985).
7. R. Sayre. J. Am. Chem. Soc. **77**, 6689 (1955) and refs. therein.
8. E.G. Samsel, K. Srinivasan, and J.K. Kochi. J. Am. Chem. Soc. **107**, 7606 (1985).
9. H. Saltzman and J.G. Sharefkin. Organic synthesis. Collected volume V. Wiley, New York. 1973. p. 658.
10. W. Agam, S. Hajra, M. Herderich, and C.R. Saha-Moller. Org. Lett. **2**, 2773 (2000).
11. R. Willoughby, E. Shechan, and S.A. Mitrovich. A global view of LC/MS: How to solve your most challenging analytical problems. Global View Publications, Pittsburgh. 1998. p. 105.
12. S.R. Logan. Fundamentals of chemical kinetics. Longman, Burnt Mill. 1996. p. 86.
13. D.G. Lee and T. Chen. J. Org. Chem. **56**, 5341 (1991).
14. D.G. Lee and H. Gai. Can. J. Chem. **73**, 49 (1995).
15. I. Fleming. Frontier orbitals and organic chemical reactions. Wiley, Chichester. 1976. p. 25–27.
16. Details of the theoretical calculations can be found in: C.R. Jackson Lepage, Ph.D. thesis, University of Regina, 2001, available through University Microfilms International or The Library, University of Regina, Regina, SK S4S 0A2, Canada.
17. E. Baciocchi, O. Lanzalunga, and S. Malandrucco. J. Am. Chem. Soc. **118**, 8973 (1996).
18. E. Baciocchi, O. Lanzalunga, and B. Pirozzi. Tetrahedron, **53**, 12287 (1997).
19. E. Baciocchi, O. Lanzalunga, and F. Marconi. Tetrahedron Lett. **35**, 9771 (1994).
20. A. Rauk. Can. Chem. News, **53(5)**, 20 (2001).
21. A. Rauk, D.A. Armstrong, and D.P. Fairlie. J. Am. Chem. Soc. **122**, 9761 (2000).
22. L.J. Marnett. Carcinogenesis, **21**, 361 (2000).
23. C.A. Bunton and N.D. Gillitt. J. Phys. Org. Chem. **15**, 29 (2002).